

# Application of DCC Targets with GOME-2 Observation for Vicarious Calibration of Visible Channels of NOAA GOES Instruments

Haifeng Qian<sup>1</sup>, Xiangqian Wu<sup>2</sup>, Fangfang Yu<sup>3</sup> and Trevor Beck<sup>2</sup>

1: I.M. Systems Group, Inc., Rockville, MD; 2: NOAA/NESDIS/STAR, College Park, MD; 3: ERT, Inc., Columbia, MD

## 1. DCC is suitable target for calibration purpose

Geostationary Operational Environmental Satellite (GOES) Imager visible channel (520–790nm) has no onboard calibration device. Although MODIS is well calibrated with sophisticated on-board calibration devices (Xiong et al, 2010), its spectral band does not match with that for GOES (Figure 1). Questions remain as to how to correct the impact from the difference between GOES and MODIS spectral response functions (SRF). Tropical deep convective clouds (DCCs) are thick, high and cold, and reflect much of the solar energy back to space, which reduces the effects of atmospheric absorption with the exception of stratospheric aerosols. Therefore, DCC is suitable as an invariant target for calibration purpose.

## 2. Methodology

**Goal and method:** We took an advantage of observation from Global Ozone Monitoring Experiment-2 (GOME-2) and Advanced Very High Resolution Radiometer (AVHRR) both onboard Metop-A satellite and applied deep convective cloud (DCC) method for vicarious calibration of visible channels of NOAA GOES instruments.

**Data:**

- Domain of interests (-180°W, 180°W, -20°S, 20°N) in 2010 ;
- GOME2 band 3 (391-607nm) and band 4 (584-798nm) measurement with its ground pixel resolution 80 km x 40 km;
- AVHRR reflectance of visible Ch1 (0.65μm) and brightness temperature from Ch4 (11 μm) from AVHRR GAC dataset (5km x 4km);
- GOES/MODIS/AVHRR Spectral Response Functions (SRF) interpolated into GOME-2 band3+4 wavelength ranges (400-790nm);
- An 8km x 8km land coverage percentage dataset originally from USGS is used to provide the global land-sea flag.

## 3. Identification of DCC' temporal and spatial variation

Firstly, DCCs identification in past studies was highly dependent on the different observing tools and sensitive to the thresholds of the observation, thus leading to uncertainties and unresolved discrepancies on DCC seasonal to interannual variation. In this study, requirements are imperative to implement to identify DCC to improve the homogeneity of GOME-2 pixels as follows:

- Median of collocated 15x13 pixels AVHRR Ch4 BT less than 205K; Standard deviation of Ch4 BT less than 10 K;
- Standard deviation of collocated 15x13 pixels AVHRR Ch1 reflectance is less than 10% of the mean reflectance.
- Overall cloud fraction is large than 90% with top cloud pressure less than 300 hpa from GOME-2 and cloud coverage flag with “cloudy” for all collocated AVHRR 13x15 pixels.

|       | DCC number | Coverage (%) | Median of Reflectance (%) | Mean of Reflectance (%) |
|-------|------------|--------------|---------------------------|-------------------------|
| < 210 | 36014      | 0.294        | 82.99                     | 82.1                    |
| < 209 | 32740      | 0.267        | 83.16                     | 82.31                   |
| < 208 | 29712      | 0.242        | 83.36                     | 82.52                   |
| < 207 | 26402      | 0.215        | 83.57                     | 82.75                   |
| < 206 | 22594      | 0.184        | 83.8                      | 83.01                   |
| < 205 | 19577      | 0.160        | 84.01                     | 83.22                   |
| < 204 | 16375      | 0.134        | 84.25                     | 83.48                   |
| < 203 | 13796      | 0.113        | 84.4                      | 83.67                   |
| < 202 | 11172      | 0.091        | 84.65                     | 83.94                   |
| < 201 | 9277       | 0.076        | 84.83                     | 84.13                   |

**Table 1.** DCC numbers, reflectance of Metop-A AVHRR Ch1 from the 15x13 pixels collocated with the GOME-2 with the thresholds of the median of AVHRR Ch4 BT in 2010;

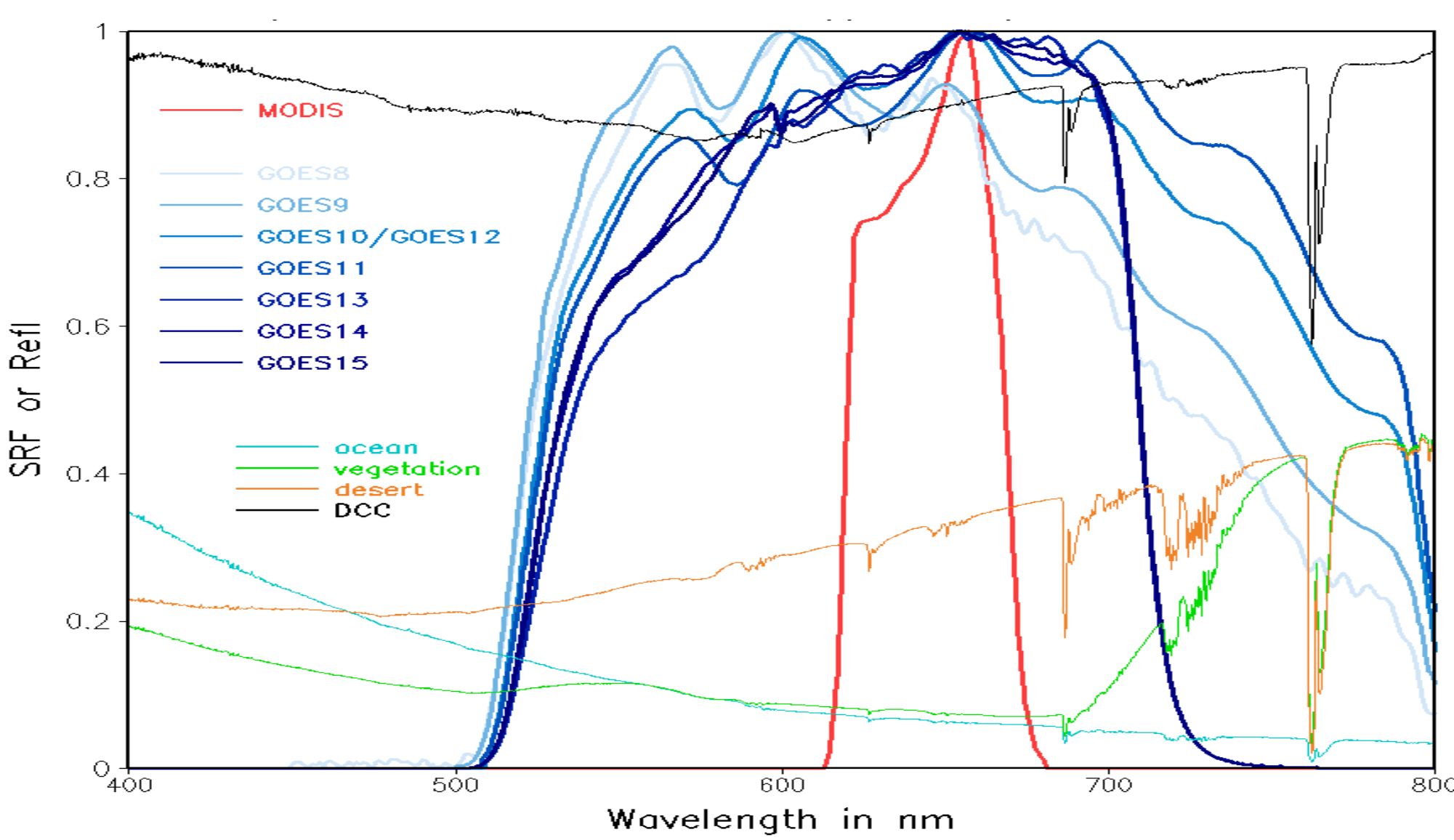


**Figure 1:** Spectral response functions for Band 1 of MODIS, visible channels of GOES-08/09/10/11/12/13/14/15. Typical types of spectral reflectance of DCC, ocean, vegetation and desert are illustrated for comparison of their characters.

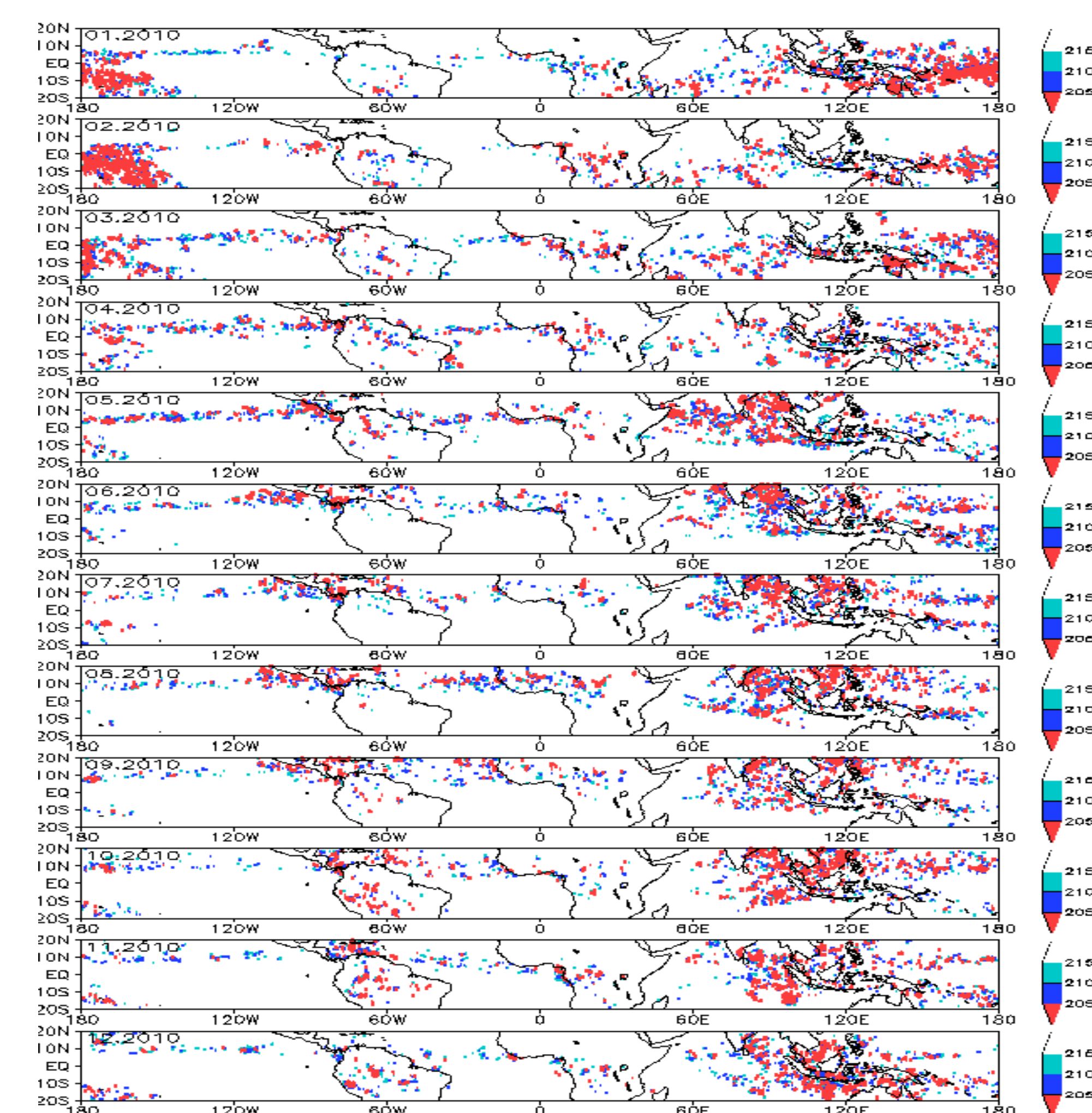


**Figure 2:** Monthly geographical distribution of DCC over 0.4° x 0.4° grids in 2010. DCCs are indicated in red with the threshold of Metop-A AVHRR BT less than 205k, and 210k, 215k are shown for reference

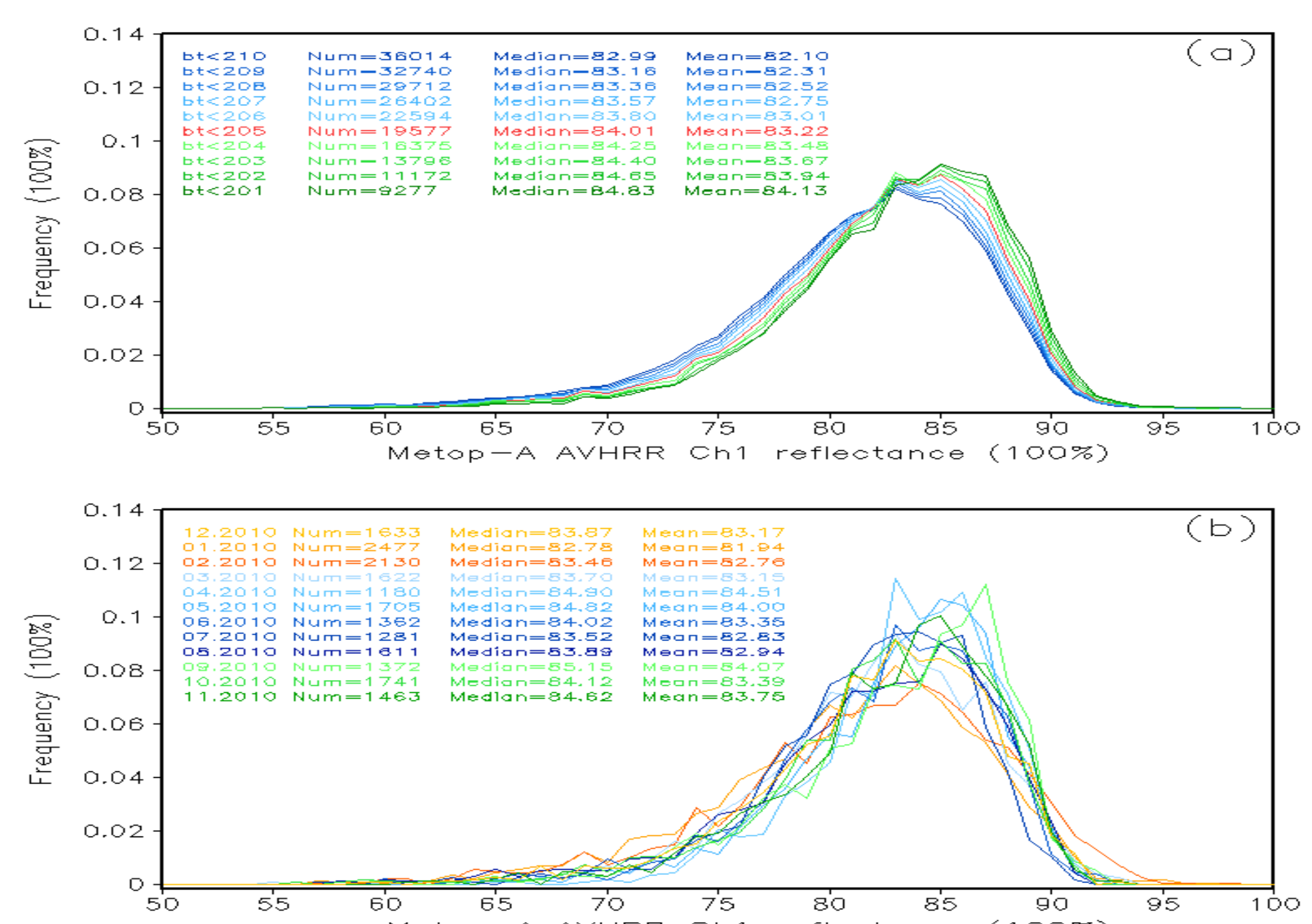


**Figure 3.** DCC PDFs of the Metop-A AVHRR Ch1 reflectance (binsize=1%) in 2010 for (a) Sensitivity of the DCC identification threshold to Metop-A AVHRR Ch4 BT; (b) each month with the threshold of Ch4 BT < 205k.

With threshold of Ch4 BT< 205K (Table 1, Figure 2-3), we identify that DCC only accounts for 0.16% of total GOME-2 pixels. Among these DCC pixels, about 10.3% located in the land and 84.6 % in the ocean. The DCC pixels on land have a large seasonal variation with moving in the tropics and subtropics. Generally, the DCC global distribution is highly related to the movement of ITCZ. A strong pronounced seasonal variation with the movement from South Hemisphere to North Hemisphere occurred in April, 2010 (Figure 2).

## 4. DCC calibration of impact of SRFs

Figure 4 indicates that about 3% of total pixels meet the cloudy condition requirement, DCC pixels account for 0.16% of total pixels. Overall, GOME-2 has roughly 12% higher than Metop-A AVHRR in all collocated pixels and narrow to 7.5% higher in DCC pixels in visible channel from the nadir subset 13/14(Figure 4 right).

The difference between GOES and MODIS reflectance is improved significantly at DCC pixels (Figure 5). For example, the difference between GOES-11 and MODIS has the largest spread. It reduced the absolute spread to 0.015 at DCC, and the mean bias close to 0 in DCC area (Figure 5a). In relative view, the spread significantly reduces from larger than 100% into less than 2% in DCC area (Figure 4d). For GOES-15, DCC calibration effectively excluded outlines pixels and shows a convergence (Figure 5b). For Metop-A, the relative difference is of higher convergence with the spread within 20% even in low reflectance. All of them indicate that in the DCC area the different is reduced and narrowed stably.

## 5. Discussion and conclusions

In this study, we used observation from GOME-2 and AVHRR both onboard Metop-A satellite to apply DCC calibration for visible channels of NOAA GOES satellite instruments. We characterize DCC temporal and spatial variation, and then investigate the spectral calibration uncertainty with DCC calibration to provide insights to improve SFR accuracy. Our analysis shows that DCC occurrence is sensitive to the thresholds with the brightness temperature (BT) of AVHRR Channel 11μm (Ch4) and its seasonal movement is largely in line with the movement ITCZ. Our analysis shows DCC from GOME-2 hyper-spectral observation is reliable as an invariant target. Results indicate that DCC method in this study helps to improve the convergence of the reflectance difference between MODIS and GOES SFRs in DCC pixels and quantify that the contribution due to SFRs difference to the bias can be narrowed to <1% (Figure 6). With this DCC calibration we suggest that the lower O<sub>2</sub> absorption may offsets the contribution from the wider right tail of GOES-11 SRF, resulting in that the contribution from GOES-11 SRF is very close to that of MODIS.

## 6. References

- Doelling, D. R., L. Nguyen, and P. Minnis, 2004: On the use of deep convective clouds to calibrate AVHRR data. *Proc. SPIE 49th Ann. Mtg.*, Earth Observing Systems IX Conf., Denver, Colorado, August 2-6, 2004
- Wu, X. M. Weinreb, I.-L. Chang, D. Crosby, C. Dean, F. Sun, and D. Han, 2005: “Calibration of GOES Imager visible channels”, *IGARSS*.
- Wu, A., X. Xiong, and C. Cao 2008, Terra and Aqua MODIS inter-comparison of three reflective solar bands using AVHRR onboard the NOAA-KLM satellites, *Int. J. Remote Sens.*, 29(7), 1997-2010.
- Xiong, X. J. Sun, X. Xie, W. Barnes, and V. Salomonson, 2010: On-Orbit Calibration and Performance of Aqua MODIS Reflective Solar Bands, *IEEE Trans. Geosci. Remote Sens.*, 48(1), 535-546.

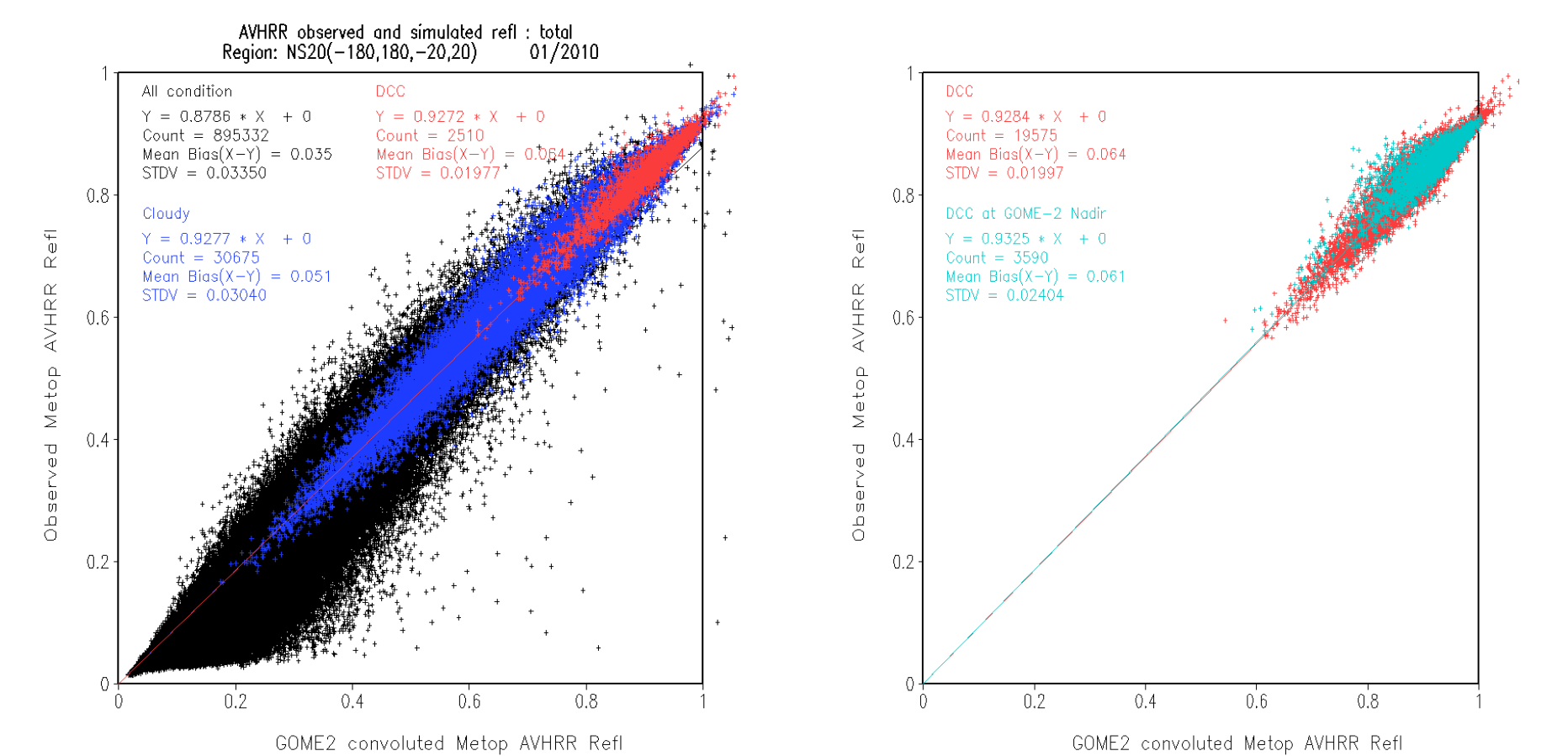


**Figure 4:** Left: Scattering of the GOME-2 convoluted Metop-A AVHRR Ch1 reflectance with the collocated AVHRR observation in 01/2010 under three conditions: 1) All collocated pixels; 2) Cloudy; 3) DCC. Right: One-year scatter diagram of the GOME-2 convoluted Metop-A AVHRR reflectance with the collocated AVHRR observation for all 2010 DCC in red and DCC at GOME-2 nadir (subset13-14) in shallow blue.

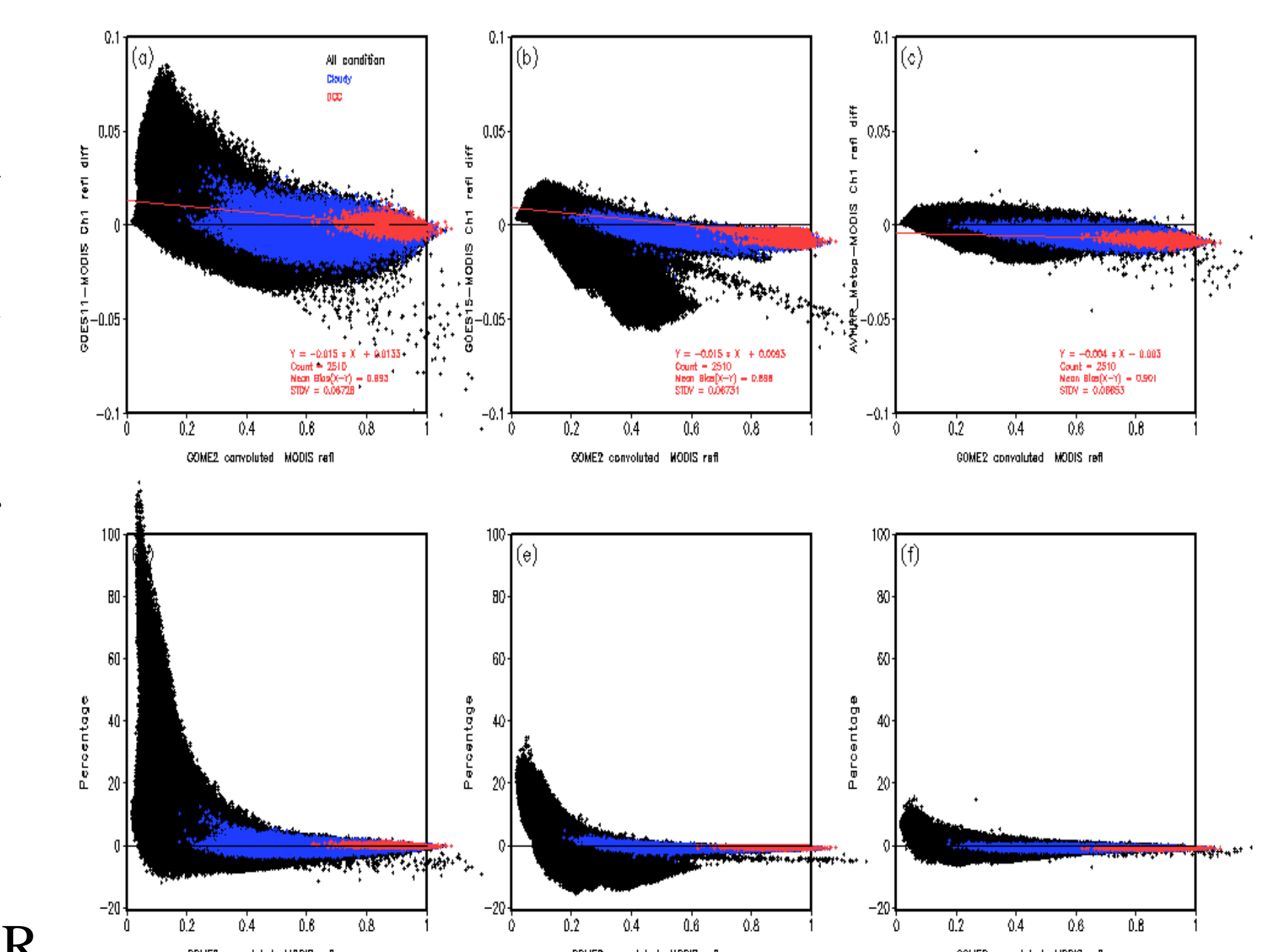


**Figure 5:** Scatter diagram of GOME-2 convoluted MODIS reflectance vs. the convoluted reflectance difference between the SFRs and MODIS in 01/2010 for (a) GOES-11; (b) GOES-15; (c) Metop-A AVHRR. Relative percentage is shown in (d) (e) (f), respectively.

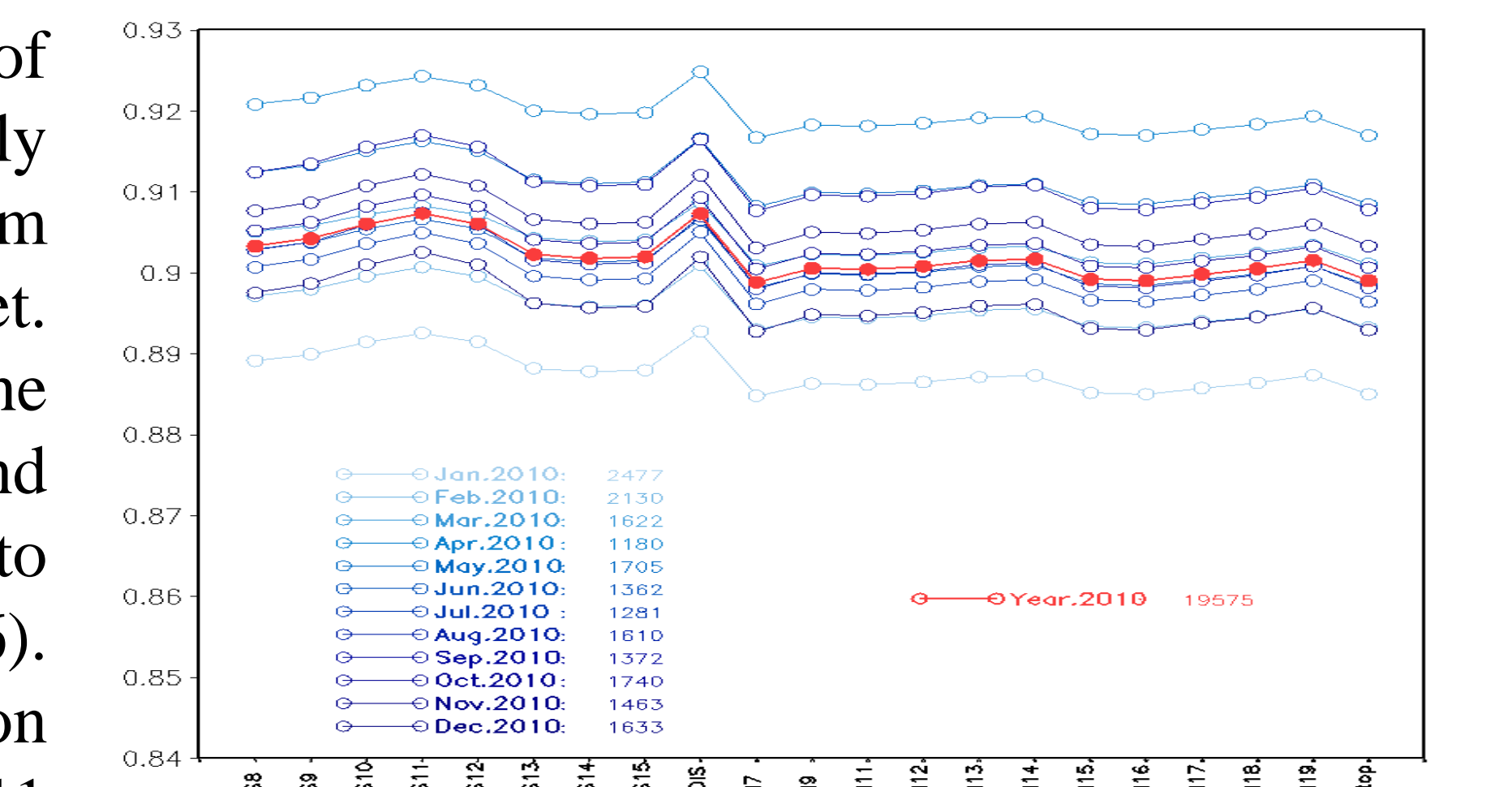


**Figure 6:** Monthly mean of convoluted reflectance for individual SFRs in 2010 (monthly ones in blue, and annual in red). The DCC numbers are counted and shown.